Preliminary determinations of geomagnetic field intensity for the last 400 kyr from the Hawaii Scientific Drilling Project core, Big Island, Hawaii

Florence Garnier, Carlo Laj, Emilio Herrero-Bervera, Catherine Kissel, Don Thomas

JOURNAL OF GEOPHYSICAL RESEARCH, VOL. 101, NO. B5, PAGES 11,665–11,673, MAY 10, 1996

Preliminary determinations of geomagnetic field intensity for the last 400 kyr from the Hawaii Scientific Drilling Project core, Big Island, Hawaii

Florence Garnier,[1] Carlo Laj,[1] Emilio Herrero-Bervera,[3] Catherine Kissel,[1] and Don M. Thomas[2]

Abstract. Preliminary paleointensity determinations using the Thelliers' method have been carried out on 141 samples of core HSDP (Hawaii Scientific Drilling Project), drilled into the Mauna Loa and Mauna Kea volcanoes and spanning the last 400 kyr. Rock magnetic investigations identify pseudo-single-domain magnetite as the main carrier of the natural remanent magnetization (NRM) all along the core. In the Mauna Kea sequence ~75% of the specimens yielded exploitable results with linear NRM/TRM (Thermoremanent Magnetization) plots and positive partial TRM (pTRM) checks generally up to the highest temperatures (550°C). A lower percentage of successful experiments (~50%) was observed for the Mauna Loa samples and the NRM/TRM diagrams are linear over a shorter temperature interval than for the Mauna Kea samples. These preliminary results, based on only one sample per flow, document a marked geomagnetic field intensity low at about 40 kyr probably related to the Laschamp event. They also suggest that the geomagnetic field at Hawaii might be characterized by large, sharp intensity fluctuations spaced by a few thousand years. The average value of the field intensity suggested by these results for the last 400,000 years is slightly higher than the present field at Hawaii.

Introduction

The 1-km core obtained near Hilo by the Hawaii Scientific Drilling Project (HSDP) [*Hawaii Scientific Drilling Project*, 1994] penetrates 196 basaltic flow units of the Mauna Loa and Mauna Kea sequences. Given the high extrusion rate of the Hawaiian volcanoes, this core provides a unique opportunity to obtain a detailed record of changes of the geomagnetic field intensity during the last few hundred thousand years.

Volcanic records of geomagnetic field changes are not as continuous as sedimentary records. However, contrary to sediments, the processes by which the magnetization of a lava was acquired is relatively well understood and can be reliably reproduced in the laboratory. It is therefore possible to obtain determinations of the absolute field intensity by comparison with a known field in the laboratory, while only relative changes of the field intensity can be obtained from sediments.

The purpose of this study is to use the sequence provided by the HSDP core to construct a record of the geomagnetic field intensity in Hawaii with better temporal continuity and accuracy than previous studies. Initial studies suggested that the Central Pacific has been a region of very low nondipole field for the past ~0.7 m.y. [*Cox and Doell*, 1964; *Doell and Cox*, 1965, 1971, 1972; *Doell*, 1969]. More recent paleomagnetic studies with better age control have shown that these first results did not yield a realistic picture of the variability of the geomagnetic field [*Coe et al.*, 1978; *Tanaka and Kono*, 1991; *Mankinen and Champion*, 1993a,b]. The new results suggest that the nondipole field might indeed have been negligible in the interval between 12 kyr and 5 kyr but that a significant nondipole field existed at Hawaii from about 5 ka to perhaps as recently as 200 years B.P. [*Coe et al.*, 1978; *Mankinen and Champion*, 1993a,b]. No new results, however, have been obtained for older periods.

We report here on the first paleointensity determinations obtained from 141 lava flows sampled over the entire length of core HSDP. Because of the time-consuming aspects of the *Thellier and Thellier* [1959] method which we have used, it has not been possible to obtain more determinations so far. Therefore these results, based on only one sample per flow, are very preliminary. Nevertheless, given the unusually high percentage of successful determinations and the high extrusion rate, they allow some new insights into geomagnetic field changes at Hawaii.

In addition, the presence of high-amplitude, short-lived fluctuations in the intensity record described below, might prove useful as a stratigraphic correlation tool on a local scale, by providing a set of high resolution time points between cores.

Sampling

Based on the core logging [*Hawaii Scientific Drilling Project*, 1994], six samples (25-mm diameter) were drilled in 196 flows using an electric drill equipped with a diamond brass barrel. The samples were drilled perpendicular to the core axis, at random azimuths due to the azimuthally unoriented nature of the core. When continuous sections of the core were

[1]Centre des Faibles Radioactivités, Laboratoire mixte Commissariat à l'Energie Atomique, Centre National de la Recherche Scientifique, Gif-sur-Yvette, France
[2]Hawaii Institute of Geophysics and Planetology, University of Hawaii at Manoa, Honolulu.

Paper number 95JB03844.
0148-0227/96/95JB-03844$05.00

encountered, samples were drilled with the same azimuth. Five samples per flow were used for the determination of the direction of the remanent magnetization [*Holt et al.*, this issue]. Only one sample per flow was dedicated to the paleointensity determinations. At the Centre des Faibles Radioactivités (CFR), each sample was cut half the size of standard paleomagnetic samples (25x11 mm) to use part of the available material for the study of the magnetic mineralogy. End chips were also used for these studies.

Temporal Framework

The different age determinations which have been used here to reconstruct the changes of the geomagnetic field intensity are summarized in Table 1. A radiocarbon date of ~40 ka has been obtained on a humic ashy soil at the 182 m depth [*Beeson et al.*, this issue]. Ar/Ar and K/Ar radiometric dating have been difficult in most cases because of the low yields of radiogenic $^{40}Ar^*$ ($1x10^{-15}$ mol) at each temperature step, masked by 20 to 50 times more atmospheric argon, and of the very low K contents due to the tholeitic composition of the basalts. Nevertheless, nine age determinations have been obtained. Seven Ar/Ar dates ranging from (107±27) to (391±40) kyr were obtained for lava flows distributed down the total length of the core. Two intermediate K/Ar ages of (352±105) and of (378±109) kyr were also obtained for flows at 720 m (flow 147) and at 799 m (flow 164), respectively. The description of these results is given elsewhere [*Sharp et al.*, this issue]. We have used this time frame (Table 1) for the interpretation of the paleointensity results.

Rock Magnetic Characteristics

Rock magnetic investigations were carried out on at least one sample every second flow to identify the magnetic carriers of the natural remanent magnetization (NRM) and the changes in magnetic mineralogy induced by heating. We have systematically performed high field thermomagnetic analyses on small amounts of powder from every flow using a horizontal Curie balance in an argon atmosphere to minimize oxidation of the magnetic minerals during the experiments. Heating and cooling rates were close to 7-8°C/min, and the maximum temperature reached was 700°C in fields of the order of 700-900 mT. Thermomagnetic experiments allow us to distinguish two main groups of samples (Figure 1).

Table 1. Radiometric Ages of Samples From Different Horizons of the HSDP Core

N°Sample ~ N°Unit	Depth(m)	Age ± err (kyr)	Radiometric Method
24	182	40 ± 3	^{14}C
43	268	107 ± 27	Ar/Ar
49	299	232 ± 4	Ar/Ar
57	325	232 ± 4	Ar/Ar
58	335	241 ± 5	Ar/Ar
75	415	325 ± 23	Ar/Ar
147	720	352 ± 105	K/Ar
164	799	378 ± 109	K/Ar
196	930	400 ± 26	Ar/Ar
211	995	391 ± 40	Ar/Ar

From *Beeson et al.* [this issue] and *Sharp et al.* [this issue].

The first group, which we have called the a type, comprising over 80% of the Mauna Kea samples, is characterized by a concave-down thermomagnetic curve continuously decreasing to zero with a single Curie temperature, close to 580°C, typical of low Ti content magnetite. In some cases, the heating and the cooling curves are perfectly reversible. More typically, however (~60% of the cases), a slightly nonreversible character of the thermomagnetic analysis reveals that the magnetic minerals have undergone some changes during the heating. Differences in the heating and cooling curves never exceed 10%, so the changes are quite small. Oxygen, which is always present in the powdered samples and in the measuring cell despite the argon flow, may be responsible for oxidation in this fraction of the samples. Two examples of a type thermomagnetic behaviors are shown in Figure 1a.

A second group of samples (which we refer to as b type) is characterized by thermomagnetic curves showing a regular decrease of the induced magnetization until 300-350°C, where transformations appear. At higher temperature, the only remaining phase is magnetite as shown by the Curie temperature (580°C) at the end of the heating. B type samples are most commonly encountered in the Mauna Loa sequence of the HSDP core. An example of a b type thermomagnetic curve is shown in Figure 1b.

Magnetic hysteresis parameters were determined on small chips with an alternating gradient force magnetometer (Micromag). The slope at high fields, which represents the paramagnetic contribution, is calculated automatically using the software provided with the instrument. The saturation remanent magnetization (Mr), the saturation magnetization (Ms), and the coercive force (Hc) were calculated after removal of this component. By applying progressively increasing back fields after saturation, we determined the coercivity of the remanence (Hcr) and the S ratio defined as S=IRM(-0.3T) /IRM(1T) [*King and Channell*, 1991]. The results document low values of Hc and Hcr and also a S ratio higher than 0.9 along the core. This indicates that a very large fraction of the NRM is carried by low-coercivity minerals, in agreement with the presence of magnetites. The ratios of the hysteresis parameters plotted as a Day diagram [*Day et al.*, 1977] in Figure 1c show that the grain size of magnetite is characterized by significant dispersion in the pseudo-single-domain range.

Directional Data

Reliable, thermally cleaned, determinations of the inclination of the characteristic remanent magnetization (ChRM) were reconstructed from successful Thellier experiments using the half vectorial sum of the magnetization vectors obtained after direct and reverse heating at each thermal step. However, the bulk of the directional data was obtained using alternating field (AF) demagnetization on several samples per flow, and is presented elsewhere [*Holt et al.*, this issue]. The direction of the (ChRM) studied so far (105 exploitable results) is consistent with these results. Most of the Zijderveld diagrams document a small viscous component easily removed at 150-180°C. Then the magnetization decreases regularly to the origin with a stable direction which could thus be accurately defined. Because the core is not azimuthally oriented, only inclination data are meaningful (Table 2).

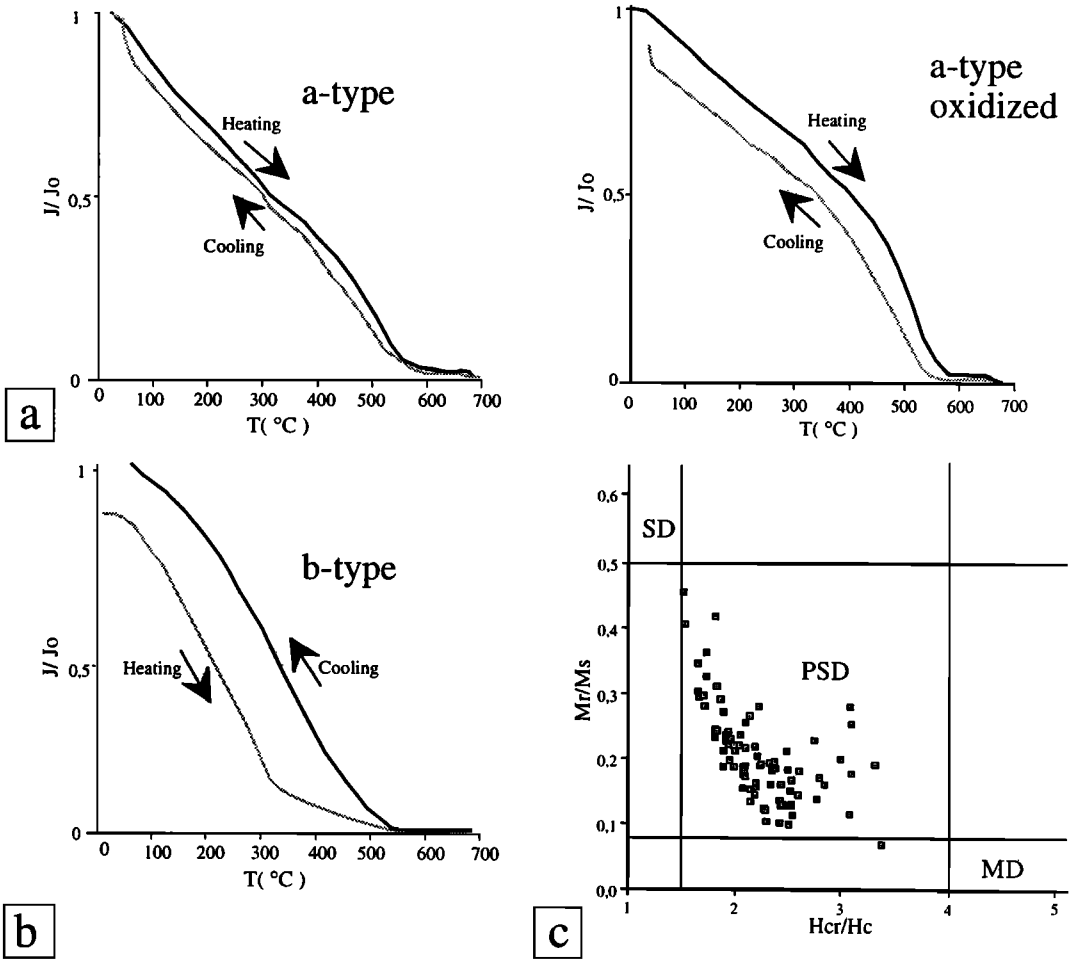

Figure 1. (a) and (b) Representative thermomagnetic analyses plots obtained using a horizontal Curie balance in an argon atmosphere. The two main types of diagrams observed are described in the text. (c) Hysteresis parameters reported on Day diagram [*Day et al.*, 1977] indicate that the size of the magnetic grains are largely dispersed in the pseudo-single domain region.

For the first 850 m (Figure 2), inclinations are generally consistent with the present-day field inclination value in Hawaii (~35°) except for a well-defined minimum at 300 m. Also, three samples located at 464, 683 and 827 m (flows 90, 140, and 168) are characterized by low inclinations (-3°, 6°, and 4°, respectively). In the lower part of the core, low inclinations are observed between 863 and 941 m (flows 173 to 196) and between 980 and 1010 m (flows 206 to 218). The inclination anomalies are defined by several measurements on successive flows which is an argument supporting the hypothesis of real geomagnetic field behaviour.

Paleointensity Determinations

Method and Data Analysis

Paleointensity determinations were performed on 141 lava flows (17 from Mauna Loa, 124 from Mauna Kea) at depths from 12 to 1049 m. The original method of *Thellier and Thellier* [1959] was employed throughout. The samples were heated twice (direct and reverse positions) from room temperature to over 550°C with at least 11 steps of amplitude 30°C to 50°C depending on the samples and the temperature range.The paleointensity furnace at the CFR has a large internal diameter allowing the simultaneous treatment of up to 80 samples. Heating of the samples lasted from 2 to 4 hours depending on the temperature, and the samples were allowed to cool naturally overnight. During the experiments an argon atmosphere was permanently kept in the furnace in order to minimize oxidation of the magnetic minerals. A field of 40 μT, close to the present field intensity in Hawaii, was applied along the z axis of the samples during both heating and cooling as suggested by *Levi* [1975]. At each step, the total magnetization was measured with a JR5-A spinner magnetometer. The magnetic stability of the samples during the experiments was tested by redetermining the partial thermal remanent magnetization (pTRM) at a given low-temperature interval after previous heating at higher temperature. The automatic temperature control of the furnace allows a given temperature to be reproduced within 1-2°C. PTRM checks could therefore be made very accurately every two temperature steps.

Paleointensity data are usually reported on a NRM/TRM diagram [*Nagata et al.*, 1963] in which the residual natural remanent magnetization (NRM) is plotted versus the associated acquired thermoremanent magnetization (TRM). Both NRM and TRM values are normalized to the value of the

Table 2. Paleointensity Determinations for Core HSDP

Sample ~ Unit	Depth,m	*f*	*g*	*q*	Fe, μT	±s.d.(Fe)	VDM, 10^{22} A m^2	±s.d.(VDM)	*I*, deg
001	12.64	0.94	0.58	10.6	47.31	2.45	11.27	0.58	28.8
011	59.22	0.56	0.73	8.9	38.48	1.79	8.26	0.38	41.5
014	107.21	0.49	0.72	13.1	39.84	1.09	9.99	0.27	19.8
015	121.00	0.32	0.75	2.8	51.89	4.58	13.04	1.15	19.2
016	138.32	0.20	0.68	2.9	53.25	2.65	10.97	0.55	45.6
020	159.94	0.34	0.79	2.7	42.26	4.24	7.72	0.77	55.9
029	200.24	0.23	0.75	2.1	15.17	0.72	3.46	0.16	34 9
034	220.81	0.53	0.79	4.9	27.52	2.36	6.75	0.58	23 9
043	266.82	0.38	0.73	7.1	31.33	1.23	6.75	0.27	41.1
046	284.37	0.35	0.77	3.5	45.27	3.56	10.84	0.85	27.9
049	300.99	0.44	0.71	1.6	54.17	10.6	13.96	2.73	12.1
050	303.76	0.33	0.75	3.1	58.53	4.81	15.10	1.24	11 9
052	309.34	0.23	0.69	1.4	53.45	3.73	13.67	0.95	14.7
057	326.76	0.54	0.85	6.7	59.02	4.06	13.56	0.93	33.8
059	345.25	0.27	0.49	6.6	44.86	2 7	10.18	0.61	35.3
060	347.10	0.42	0.75	9.9	44.28	1.42	10 28	0.33	32.4
061	349.53	0.58	0.79	5.3	43.09	3.75	9.21	0.80	41.9
065	372.33	0.47	0.85	12.2	38.43	1.26	8.05	0.26	43.9
068	376.89	0.53	0.76	9.9	58.75	2.37	12.49	0.50	42.5
069	379.29	0.40	0.77	7.1	29 15	1.29	6.86	0.30	30.5
071	394.64	0.34	0.74	4.6	40.05	2.27	8.25	0.47	45.6
073	407.72	0.31	0.77	6.9	29.45	1.02	5.84	0.20	49.1
075	418.24	0.28	0.75	2.3	25.05	2.37	6.11	0.58	25.0
076	422.72	0.38	0.78	5.3	46.77	2.67	9.39	0.54	47.9
078	430.76	0.33	0.78	6.8	43.55	1.66	9.10	0.35	44.3
080	434.44	0.27	0.56	0.6	68.99	11.1	12.55	2.02	56.2
082	440.10	0.53	0.79	3.9	39	4.22	9.62	1.04	22.9
088	449.27	0.53	0.74	5.2	31.18	2.38	6.83	0.52	39.3
090	464.13	0.30	0.74	4.4	24.71	1.25	6.47	0.33	-2.8
091	472.42	0.57	0.68	10.3	61.7	2.34	14.93	0.57	26.3
094	481.06	0.24	0.74	7.6	38.95	0 94	9.33	0.23	28 0
096	486.34	0.43	0.67	10.7	43.75	1.18	10.27	0.28	30.9
098	494.22	0.35	0.7	6.9	29.37	1.07	7.14	0.26	25.6
099	500.86	0.53	0.75	15.3	33.68	0.88	7.92	0.21	30 7
100	505.01	0.25	0.73	4.3	44.41	1.88	8.88	0.38	48.3
102	508.21	0.51	0.56	6.2	61.41	2.86	14.84	0.69	26 6
103	513.80	0.74	0.71	12.9	49.65	2 03	10.86	0.44	39.5
104	516.83	0.25	0.73	1.7	38.8	2.6	8.58	0.57	38 3
106	527.33	0.43	0.79	13.6	57.69	1.45	12.45	0.31	41.0
107	531.62	0.50	0.75	10.8	45.9	1.61	9.62	0.34	43.9
108	539.4	0.37	0.76	3.8	43.76	3.34	10.77	0.82	23.5
110	547.08	0.52	0.71	9.5	39 38	1.53	9.58	0.37	25.4
111	553.89	0.31	0.26	3.5	41.3	0.96	10.15	0.24	23.6
112	557.02	0.65	0.76	43	45.88	0.88	11.21	0.21	24.8
114	566.45	0.25	0.68	1.3	73.62	6.01	17.89	1.46	25.6
116	572.31	0.23	0.63	0.5	33.33	1.45	8.54	0.37	14.2
119	597.70	0.36	0.58	2.7	43.63	3.35	10.74	0.82	23.4
120	604.65	0.63	0.82	13.3	40.07	1.57	8.33	0.33	44.7
123	609.26	0.27	0.47	1.9	45.86	1.97	9.54	0.41	44 7
126	627.12	0.59	0.75	8.0	44.45	2.48	11.16	0.62	19.3
129	636 88	0.49	0.85	7.8	66.3	3.61	16.05	0.87	26.3
130	643.09	0.61	0.73	10.6	40.1	1.7	9.09	0.39	35.4
131	645.57	0.32	0.75	6 5	48.28	1.81	10.63	0.40	38.8
134	661.96	0.31	0.8	4.9	39.35	2.01	9.24	0.47	30.9
135	662 81	0.27	0.67	2.7	35.89	2.5	8.49	0.59	29.8
136	665.95	0.38	0.65	6.7	54.04	2.04	13.30	0.50	23.4
138	677.03	0.36	0.81	3 8	56.61	4.42	12.50	0.98	38.5
140	683.58	0.22	0.74	5.6	48 16	1.43	12.57	0.37	6.2
142	697.66	0.38	0.79	6.3	53.95	2 59	13.64	0.65	17 7
143	700.56	0.34	0.68	5.7	67.94	2.85	15.74	0.66	32.7
144	705.41	0.36	0.86	4.4	70.73	5.02	14.42	1.02	46.5
147	721.82	0.28	0.75	3.0	37.23	2.64	7.57	0.54	46.8
148	723.99	0.49	0.58	7.1	62.37	2.55	12.89	0.53	45.3
149	725.48	0.21	0.61	3.2	40	1.62	9.87	0.40	22.9
151	737.50	0.21	0.76	2.4	34.51	2.37	8.02	0.55	32.2
152	741.55	0.57	0.74	13.4	38.25	1.22	8.81	0.28	33.5
153	748.55	0.34	0.82	7.3	41.95	1.64	9.99	0.39	28.9
156	766.32	0.22	0.52	1.4	35.33	1.68	8.45	0.40	28.3
158	775.51	0.53	0.81	10.9	44.35	1.79	8.43	0.34	52.6
160	791.29	0.23	0.75	4.4	53.85	2.2	11.12	0.45	45.3

Table 2. (continued)

Sample ~ Unit	Depth,m	*f*	*g*	*q*	Fe, μT	±s.d.(Fe)	VDM, 10^{22} A m^2	±s.d.(VDM)	*I*, deg
161	792.02	0.37	0.72	1.2	53.55	5.65	10.91	1.15	46 6
165	809.03	0.87	0.85	19.9	30.77	1.14	6.74	0.25	39.3
166	817.60	0.35	0.76	2.4	70.71	2.45	16.54	0.57	31.4
168	826.62	0.35	0.7	2.8	49.33	4.35	12.91	1.14	3.6
169	830.06	0.35	0.77	3.1	62.6	2.39	12.91	0.49	45.5
172	846.22	0.26	0.72	0.7	31.83	2.19	5.70	0.39	57 5
173	863.09	0.43	0.78	4.8	52.99	3.79	12.92	0.92	25.1
174	866.65	0 37	0.77	3.1	41.79	3 92	10.55	0 99	18.2
177	875.26	0.20	0.76	3 3	47.77	2.25	11.65	0 55	25 1
178	880.43	0.54	0.5	6.4	38.86	1.68	9.98	0.43	13.4
179	885.57	0.59	0.77	12	51.3	1 96	13.14	0 50	14 2
181	887.93	0.24	0.73	2.9	38.13	2.4	9.97	0.63	4.7
182	891.59	0.29	0.71	1.3	31.42	1.56	8.18	0.41	7.6
184	895.11	0.38	0.77	4.7	33.51	1.02	8.71	0.26	8.9
188	908.54	0.39	0 71	4.1	52.8	3.55	13.56	0.91	13 3
190	922.10	0.29	0.76	4.6	61.05	3	15.02	0.74	23.5
191	924.89	0.46	0.78	9 8	40.85	1 53	9.69	0 36	29.4
193	926.70	0.31	0 75	4.7	35.02	1.79	8.79	0.45	19.5
196	941.38	0.31	0.76	0.4	40.01	7 06	9.52	1.68	29 1
197	947.38	0.25	0.82	2.7	43.98	3.46	9 86	0.78	36.7
199	954.17	0.25	0.61	0.9	26.63	2.58	6.26	0.61	30.8
200	956.74	0.32	0.8	4.9	20.73	1.07	5.06	0.26	24.8
201	959.88	0 43	0.6	13.4	21.72	0.42	5.16	0.10	29.3
203	965.11	0.41	0.8	5.9	42.39	2.35	9.27	0.51	39.5
204	973.15	0.29	0.77	2.9	28.33	1.47	6 19	0.32	39.7
206	980.07	0.30	0.55	4.6	30.33	1.11	7.50	0.27	22.5
208	985.49	0.59	0.77	22.3	36.91	0.76	8.71	0.18	30 3
209	988.87	0.34	0.7	7.3	31.46	1.04	7.79	0.26	22.2
211	995.61	0.42	0.78	10.5	27.39	0.85	6.99	0.22	15.5
214	1000.51	0.28	0.75	3.0	35.13	2.53	9.16	0.66	6.5
218	1011.45	0.50	0.82	5.3	49.56	3.96	12.08	0.97	25.2
220	1025.30	0.25	0.81	3	47.5	3.29	10.19	0.71	41.6
221	1031.18	0.28	0.79	1.8	65.19	5 23	15.30	1.23	30.9
222	1033.09	0 39	0 75	1.9	24.28	1.82	5.37	0.40	38 2
226	1049.94	0.31	0.84	11.1	16.53	0.39	3.73	0.09	35.9

The inclination *I* is positive downward; *f*, *g*, and *q* are the NRM fraction, gap factor, and quality factor, respectively [*Coe et al.*, 1978]; Fe is the paleointensity estimate for an individual specimen, and s.d.(Fe) is its standard deviation [*Prevot et al.*, 1985], VDM is the virtual dipole moment.

NRM at room temperature. In an ideal diagram all the NRM/TRM points fall on a straight line, the slope of which gives the ratio between the applied laboratory field and the Earth's paleofield. In practice, because oxidation processes and magnetochemical changes due to heating are difficult to avoid completely during the experiment, only part of the diagram can be used for reliable paleointensity estimates. Following the suggestion of *Coe et al.* [1978], slopes defined by less than four points and corresponding to the removal of less than 15% of the total NRM were not used for paleointensity determinations. The highest temperature which was considered as reliable is the temperature at which magnetochemical transformations begin to occur, as illustrated by nonlinearity in the NRM/TRM curve and negative pTRM checks, i.e., when the new pTRM value at a given temperature differ by more than 5% from the previous one [*Coe*, 1967]. Paleointensity was then calculated using a least squares fitting on a straight line through the data in the selected temperature interval.

Finally, the overall quality of the paleointensity estimates was evaluated using the statistical parameters developed by *Coe et al.* [1978]. The NRM fraction f is the percentage of the NRM taken into account for the determination. The gap factor g is a measure of how the NRM/TRM points are distributed along the straight-line segment. The more irregular the spacing between the selected points of the segment, the more g will decrease from unity. The assessment of quality q is a function of these parameters (q=bfg/s(b)), where b is the slope of the straight line and s(b) is the standard error of the slope.

Results of the Thellier Experiments

A total of 96 samples (out of 124) from the Mauna Kea volcano and 9 samples (out of 17) from Mauna Loa yielded exploitable diagrams. The results are reported in Table 2 with the associated statistical parameters. Typical examples are shown on Figure 3 where the NRM/TRM diagrams are reported on the left and the associated demagnetization diagrams on the right. Samples which were judged unsuitable for determining the paleointensity show magnetochemical changes at very low temperature as evidenced by failure of the pTRM checks and very unstable directional behavior.

Among the Mauna Kea samples, the highest percentage of reliable diagrams was obtained from samples characterized by a-type thermomagnetic curves, consistent with the

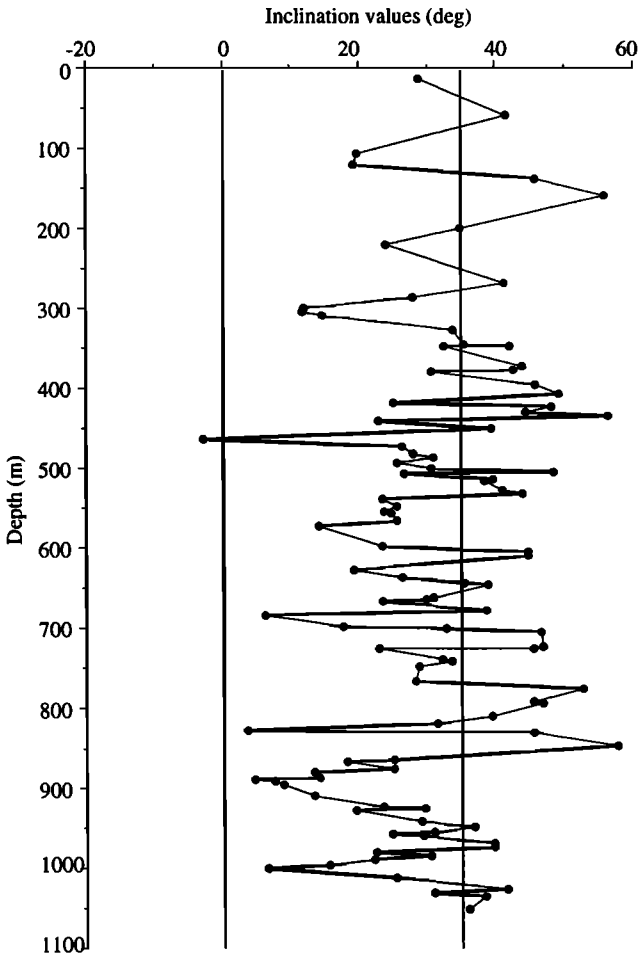

Figure 2. Overall inclination record derived from the *Thellier and Thellier* [1959] experiments versus depth, showing lower inclination values in the bottom of the core. The dashed horizontal line is the present-day inclination value in Hawaii.

observations of other authors [*Coe et al.*, 1978; *Mankinen and Champion*, 1993a,b]. A representative result obtained from this group of samples is shown in Figure 3a. Except for the first point illustrating a small secondary component present at room temperature, the NRM/TRM diagram shows a perfect straight line documented by several steps of heating. The pTRM checks are perfectly reliable through the entire temperature cycle up to 430-550°C. The reconstructed demagnetization diagram identifies a single magnetization component in good correspondence with the NRM/TRM diagrams. Such results were obtained from 69 samples of the Mauna Kea volcano and thus represent the majority of the successful determinations.

The other 27 exploitable Thellier experiments from the Mauna Kea sequence were obtained from b-type samples. In this case, as shown in Figure 3b, the first part of the NRM/TRM diagram is linear with one or two successfull pTRM checks up to 300-350°C. From this temperature, which corresponds to the removal of about 50% of the NRM, a change in the slope is observed in the diagrams and the points lie above the extrapolation of the low-temperature trend (Figure 3b). Also the pTRM checks are no longer positive. As remarked by *Coe et al.* [1978], irreversible changes in the NRM and TRM spectra severely increase with the temperature to which the specimen is heated. A low-temperature segment is thus usually more trustworthy for reliable estimates of paleointensity than high-temperature segments of diagrams of comparable quality. In b-type samples from Mauna Kea, the change in the NRM/TRM slope occurs at the same temperature as the mineralogical transformation observed from thermomagnetic experiment. We thus believe that the first part of the diagram is representative of the primary magnetization, which is confirmed by a stable behavior on the demagnetization diagram. We have thus based our paleointensity estimates on the 100°C to 350°C temperature interval.

For Mauna Loa, only nine samples are characterized by linear NRM/TRM diagrams and positive pTRM checks between room temperature and about 350°C (Figure 3c). From this temperature, which corresponds to a destruction of about 70-80% of the NRM intensity, and in agreement with the b-type thermomagnetic behavior, the data points deviate from the regression line and negative PTRM checks indicate mineralogic changes upon heating. On the basis of these preliminary results, Mauna Loa samples do not appear as favorable as those from the Mauna Kea for paleointensity studies.

From a statistical point of view, the proportion of the NRM removed during the "successful" fraction in these experiments ranges from ~20 to ~90%. G values shown in Table 2, and NRM/TRM diagrams presented in Figure 3, show that errors in slope determinations due to inadequate selection of the NRM spectrum are smaller than 5% on the average.

Assuming that this results document a realistic image of the geomagnetic field intensity changes, the maximum value of the field strength is 73 μT, the minimum 21 μT. The average value is ~44 μT, which is slightly, but significantly higher than the present-day field intensity in Hawaii (38 μT).

Discussion and Conclusion

As discussed above, NRM/TRM diagrams meet rather strict requirements for reliable paleointensity results. These diagrams may thus, in principle, allow a description of the geomagnetic field in Hawaii in the last 400,000 years. Many previous studies, however, have documented that significant differences (up to 30-40%) may exist in the paleointensity estimates obtained from samples from the same flow. The preliminary results obtained here must then be examined with particular caution. Clearly, replicate measurements are needed before one can claim that these data represent precise estimates of the geomagnetic field intensity in the past.

Nevertheless, some of the characteristics of the record obtained so far (Figure 4) reflect previously documented characteristics of geomagnetic field intensity in the past. For instance, the record documents a very low intensity at ~40 kyr. This is a characteristic observed in many volcanic and sedimentary records worldwide and is usually considered to be related to the Laschamp event [*Bonhommet and Babkine*, 1967; *Levi et al.*, 1987, *Roperch et al.*, 1988; *Tric et al.*, 1992; *Lehman et al.*, 1996]. This hypothesis is also supported by the low inclination values observed by *Holt et al.* [this issue] in the same period of time which fall within the paleointensity low. Future Thellier experiments on flows 23 and 32, which have not been studied yet, may help constrain

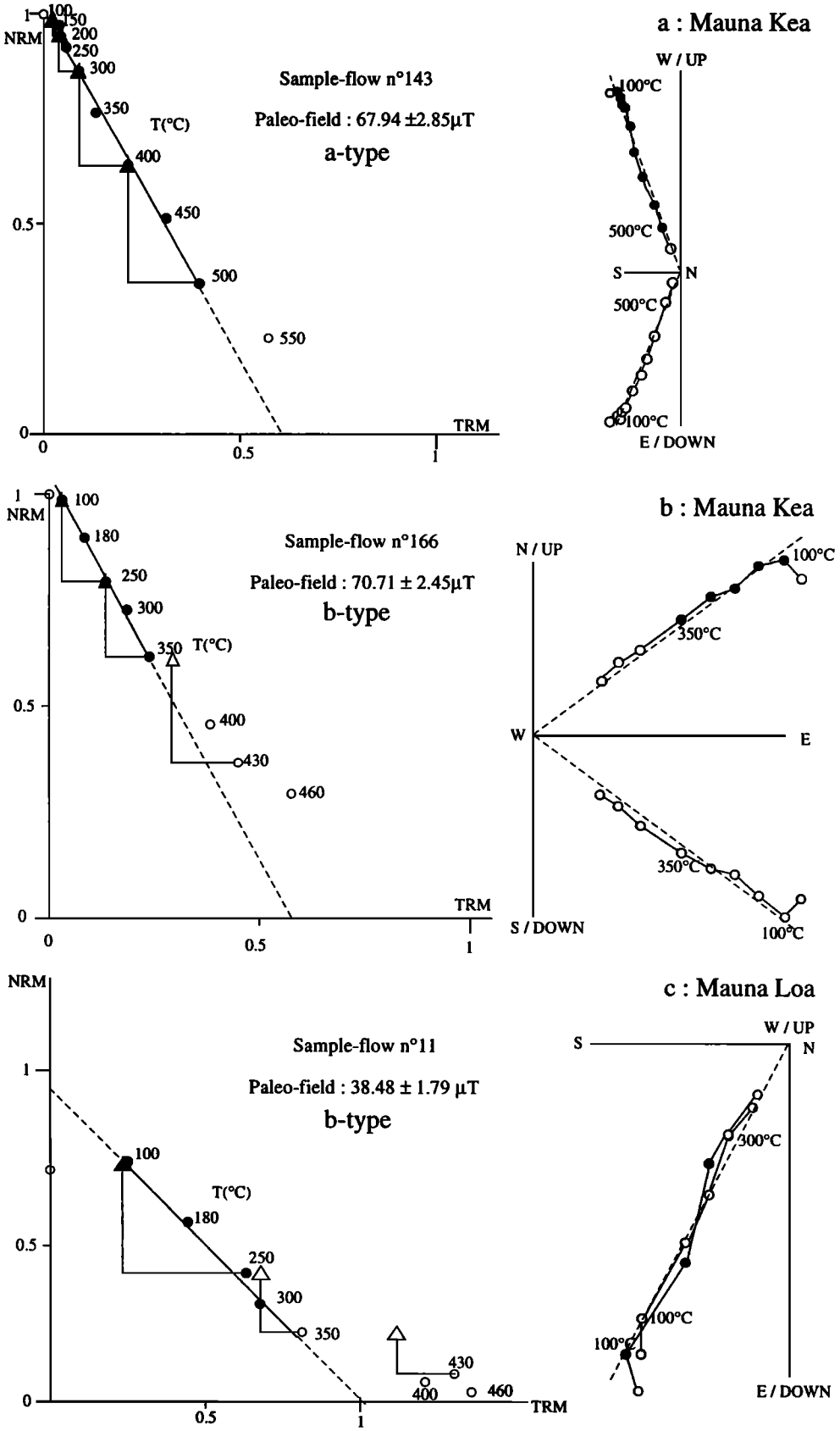

Figure 3. Three typical NRM/TRM diagrams showing paleointensity estimates obtained from the Mauna Kea and Mauna Loa volcanoes. Circles are NRM/TRM points calculated for each double heating at the temperature indicated close to the points. PTRM checks are reported with triangles. Solid symbols correspond to the part of the diagram used for the estimation of the paleointensity. The corresponding double-orthogonal projections are shown on the right side (open and solid circles are projection onto the vertical and horizontal planes, respectively).

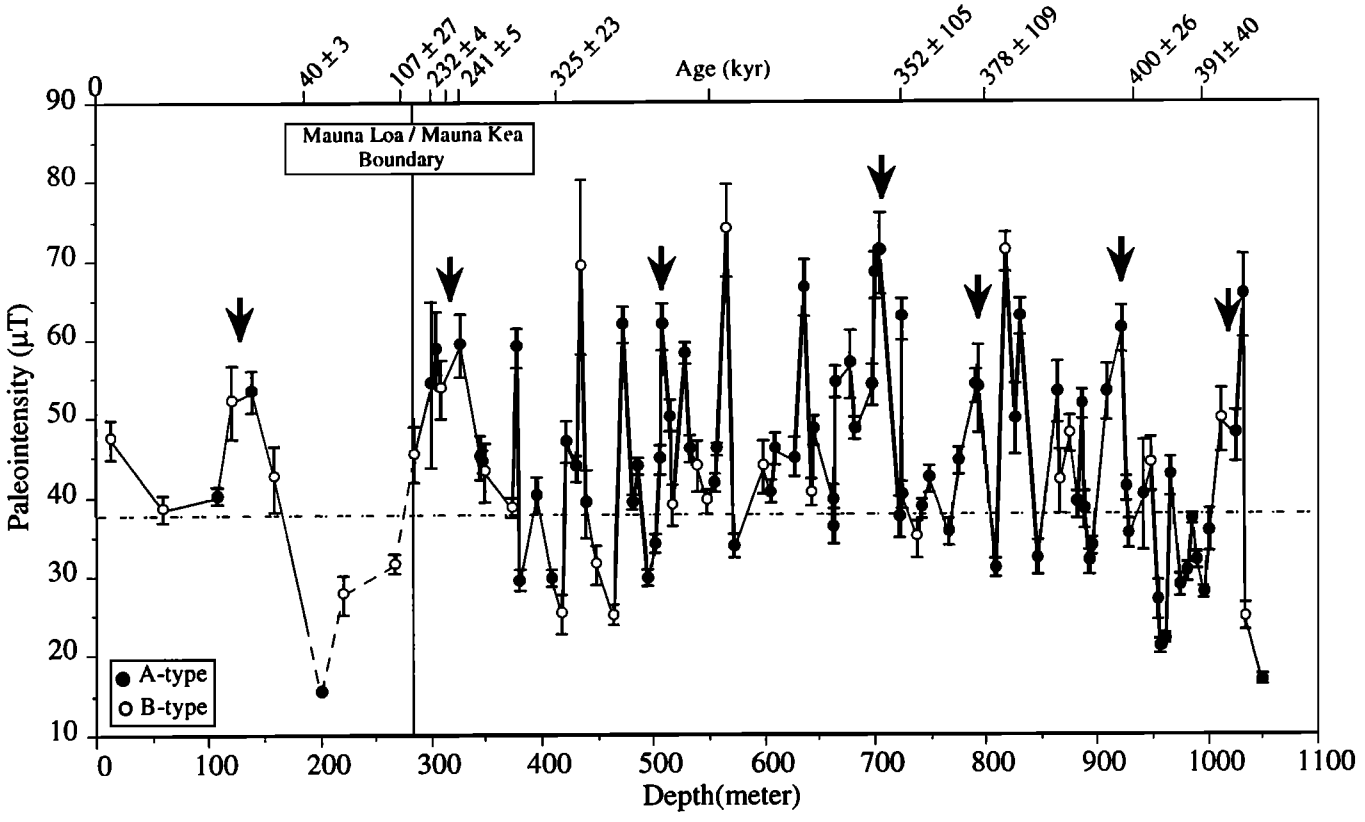

Figure 4. Paleointensity estimates as a function of depth and age for the HSDP core. Error bars indicate the error in the determination of the regression line fitting the NRM/TRM diagrams. The dashed horizontal line is the present-day field intensity in Hawaii. Solid circles correspond to the a type mineralogic behavior shown in Figure 1 and open circles correspond to the b type. Arrows indicate fluctuations defined by several points.

these results. On Hawaii, this low appears in the record obtained from the Scientific Observation Hole 4 (SOH 4) [*Garnier et al.*, 1996] which penetrated the Kilauea sequence.

The most prominent feature of the HSDP record, namely, the presence of large fast fluctuations, is also apparent in the SOH 4 record. As shown in Figure 4, some of these fluctuations appear to be defined by three to four points from successive flows which consistently document an increase then a decrease in intensity (these fluctuations are indicated by arrows in Figure 4). Others fluctuations are defined by a single point, and their amplitude of some 20 μT (i.e., a change of ~40% with respect to the mean) is of the order of magnitude of the largest fluctuations of paleointensity occasionally observed from different samples of the same flows. Although it is not likely that fluctuations of this order of magnitude are present in lava flows yielding NRM/TRM of such high quality, a spurious, nongeomagnetic origin cannot be excluded on the basis of the laboratory experiments alone. The existence of similar fluctuations in the SOH 4 record is an argument in favor of a geomagnetic origin. Although the SOH 4 record spans a different period of time than HSDP, the fluctuations observed in these two records appear to have broadly similar characteristics, i.e., they are separated by a few thousands years and have comparable amplitude.

These fluctuations are not documented in previous records of geomagnetic field intensity obtained from other regions. Very few of the earlier records, however, have the continuity and temporal resolution of the sequence sampled by the HSDP core. So it may well be that the presence of fluctuations has not been as clearly documented elsewhere because of the unique characteristics of the core. These fluctuations may reflect nondipole field changes in the proximity of Hawaii. The reality of the fluctuations defined so far by single points should be resolved by the complete study of the HSDP core now under way in our laboratory.

Acknowledgments. We thank Ed Stolper for providing the stratigraphy of the core in real time during the sampling at Caltech. John Holt helped with the sampling, and he and Joe Kirschvink are also thanked for discussions. Ed Mankinen and Jim Channell kindly read and improved the first draft and the final copy of this manuscript, respectively. We also wish to thank Scott Bogue and the second unknown referee for their many constructive remarks. F.G. gratefully acknowledge a Ph.D. grant from the Atomic Energy Commission (CEA). E.H-B. acknowledges the partial financial support from SOEST-HIGP and also from the NSF grant EAR-9508302. This is a SOEST contribution number 3998 and HIGP contribution number 858. This work has been supported in France by the CEA and by the CNRS-INSU DBT program Terre Profonde for the field trip. CNRS-INSU Terre Profonde contribution number 35 and CFR contribution number 1772.

References

Beeson, M.H., D.A. Clague and J.P. Lockwood, Origin and depositional environment of clastic deposits in the Hilo drill hole, Hawaii, *J. Geophys. Res.*, this issue.

Bonhommet, N., and J. Babkine, Sur la présence d'aimantations inversées dans la Chaîne des Puys, *C.R. Acad. Sci., Ser. B, 264*, 92, 1967.

Coe, R.S., The determination of paleo-intensities of the Earth's magnetic field with emphasis on mechanisms which could cause non-ideal behavior in Thellier's method, *J. Geomagn. Geoelectr., 19,* 157-179, 1967.

Coe, R.S., S. Grommé, and E.A. Mankinen, Geomagnetic Paleointensities from radiocarbon-dated lava flows on Hawaii and the question of the Pacific nondipole low, *J. Geophys. Res., 83,* 1740-1756, 1978.

Cox, A., and R.R. Doell, Long period variations of the geomagnetic field, *Bull. Seismol. Soc. Am , 54,* 2243-2270, 1964.

Day, R., M. Fuller, and V.A. Schmidt, Hysteresis properties of Titanomagnetites: Grain-size and compositional dependance, *Phys. Earth Planet. Inter., 13,* 260-267, 1977.

Doell, R.R., Paleomagnetism of the Kau volcanic series, Hawaii, *J. Geophys. Res., 74,* 4857-4868, 1969.

Doell, R.R., and A. Cox, Paleomagnetism of Hawaiian lava flows, *J. Geophys Res., 70,* 3377-3405, 1965.

Doell, R.R., and A. Cox, Pacific geomagnetic secular variation, *Science, 171,* 248-254, 1971.

Doell, R.R., and A. Cox, The Pacific geomagnetic secular variation anomaly and the question of lateral uniformity in the lower mantle, in *The Nature of the Solid Earth.*, edited by E.C. Robertson, pp. 245-284, McGraw-Hill, New York, 1972.

Garnier, F., C. Laj, E. Herrero-Bervera, H. Guillou, C. Kissel, and D.M. Thomas, Geomagnetic field intensity over the last 42 000 years, obtained from core SOH-4, Big Island, Hawaii, *J. Geophys. Res , 101,* 585-600, 1996

Hawaii Scientific Drilling Project, *Core-logs*, edited by E. Stolper and M. Baker, 471 pp., Calif. Inst. of Technol., Pasadena, 1994.

Holt, J.W., J.L. Kirschvink, and F. Garnier, Geomagnetic field inclinations for the past 400 kyr from the 1-km core of the Hawaii Scientific Drilling Project, *J. Geophys. Res.*, this issue.

King, J.W., and J.E.T. Channell, Sedimentary magnetism, environmental magnetism, and magnetostratigraphy, *U.S. Natl. Rep. Int. Union Geod. Geophys. 1987-1990, Rev. Geophys., 29,* 358-370, 1991.

Lehman, B., C. Laj, C. Kissel, A. Mazaud, M. Paterne and L. Labeyrie, Relative changes of the geomagnetic field intensity during the last 280 kyr from piston cores int he Açores area, *Phys. Earth Planet. Inter.*, in press, 1996.

Levi, S., Comparison of two methods of performing the Thellier experiment (or, how the Thellier method should not be done), *J. Geomagn. Geoelectr., 27,* 245-255, 1975.

Levi, S., H. Audusson, R.A. Duncan, and L. Kristjansson, The geomagnetic excursion at Skalamaelifell, Iceland: additional evidence for unstable geomagnetic behaviour circa 40 ka ago, *Eos Trans. AGU, 68,* 1249, 1987.

Mankinen, E.A., and D.E. Champion, Broad trends in geomagnetic paleointensity on Hawaii during Holocene time, *J. Geophys. Res., 98,* 7959-7976, 1993a.

Mankinen, E.A., and D.E. Champion, Latest Pleistocene and Holocene geomagnetic Paleointensity on Hawaii, *Science, 262,* 412-416, 1993b.

Nagata, T.Y., Arai, and K. Momose, Secular variation of the geomagnetic total force during the last 5000 years, *J. Geophys. Res., 68,* 5277-5282, 1963.

Prévot, M., E.A. Mankinen, R.S. Coe, and C.S. Gromme, The Steens Mountain (Oregon) geomagnetic polarity transition, 2, Field intensity variations and discussion of reversals models, *J. Geophys. Res., 90,* 10,417-10,448, 1985.

Roperch, N. Bonhommet, and S. Levi, Paleointensity of the earth's magnetic field during the Laschamp excursion and it's geomagnetic implications, *Earth Planet.Sci.Lett., 88,* 209-219, 1988.

Sharp, W.D., B.D. Turrin, P.R. Renne, and M.A. Lanphere, The $^{40}Ar/^{39}Ar$ and K/Ar dating of lavas from the Hilo 1-km core hole, Hawaii Scientific Drilling Project, *J. Geophys. Res.*, this issue.

Tanaka, H., and M. Kono, Preliminary results and reliability of paleointensity studies on historical and ^{14}C dated Hawaiian lavas, *J. Geomagn. Geoelectr., 43,* 375-388, 1991.

Thellier, E., and O. Thellier, Sur l'intensité du champ magnétique Terrestre dans le passé historique et géologique, *Ann. Géophys., 15,* 285-376, 1959.

Tric, E., J.P. Valet, P. Tucholka, M. Paterne, L. Labeyrie, F. Guichard, L. Tauxe, and M. Fontugne, Paleointensity of the geomagnetic field during the last 80,000 years, *J. Geophys. Res., 97,* 9337-9351, 1992.

F. Garnier, C. Kissel, and C. Laj, Centre des Faibles Radioactivités, Laboratoire mixte CEA-CNRS, 91198 Gif-sur-Yvette, France.(e-mail: Florence.Garnier@cfr.cnrs-gif.fr; Catherine.Kissel@cfr.cnrs-gif.fr; Carlo.Laj@cfr.cnrs-gif.fr).

E. Herrero-Bervera and D.M. Thomas, Hawaii Institute of Geophysics and Planetology, University of Hawaii, Honolulu, HI 96822. (e-mail: herrero@soest.hawaii.edu; dthomas@soest.hawaii.edu).

(Received May 1, 1995; revised December 7, 1995;
accepted December 19, 1995.)